

Supramolecular π -Stacked Assemblies of Bis(urea)-Substituted Thiophene Derivatives and Their Electronic Properties Probed with Scanning Tunneling Microscopy and Scanning Tunneling Spectroscopy

A. Gesquière, S. De Feyter, and F. C. De Schryver*

University of Leuven (KULeuven), Department of Chemistry, Laboratory of Molecular Dynamics and Spectroscopy, Celestijnenlaan 200-F, 3001 Heverlee, Belgium

F. Schoonbeek, J. van Esch, R. M. Kellogg, and B. L. Feringa

University of Groningen, Laboratory of Organic and Inorganic Molecular Chemistry, Nijenborg 4, 9747 AG Groningen, The Netherlands

Received January 30, 2001

ABSTRACT

In this contribution we investigated the two-dimensional (2D) supramolecular organization and electronic properties of two bis(urea)-substituted oligothiophene derivatives, containing two or three thiophene units (T2 and T3, respectively), at the solution/graphite interface with scanning tunneling microscopy (STM) and scanning tunneling spectroscopy (STS). Because of the π -stacking of the oligomers the observed zero conductance band gap in the $I(V)$ curves of a ribbon is found to be considerably smaller than for an isolated oligothiophene molecule, indicating that there exists an effective conjugation in the π -stacked ribbons on the surface.

With scanning tunneling microscopy (STM) the structure and physical properties of surfaces and ordered adlayers on these surfaces can be investigated with high spatial resolution. Because of the local nature of STM, it is also possible to address individual molecules and atoms with this technique. An interesting application of this quality is the probing of the electronic properties of individual molecules (atoms) with scanning tunneling spectroscopy (STS), i.e., by collecting local $I(V)$ characteristics. This method has already successfully been applied in the field of semiconductors such as silicon,¹ semiconductor surfaces and atomic adsorbates on semiconductor surfaces,² and superconductors³ and in the study of metal surfaces.⁴ Highly oriented pyrolytic graphite (HOPG) and related carbon based structures as, for example, C₆₀, C₃₆, and carbon nanotubes have been studied with STS as well.⁵

There are, however, only a limited number of examples in the literature of STS studies on organic molecules, especially at the liquid/solid interface. In the latter case this

is most probably due to the sometimes poor reproducibility, which is caused by drift, the presence of the liquid and the mobility of the adsorbates. Hence most reported STS studies were carried out under UHV conditions. Individual copper phthalocyanine (CuPc) molecules, previously researched by Gimzewski et al.,⁶ were studied further by Dekker et al.⁷ Resonant tunneling through the HOMO of CuPc was observed, giving rise to asymmetric $I(V)$ curves that show an enhanced current at negative sample bias. The band gap of the Pc was not observed, however. Similarly, orbital-mediated tunneling through the π^* LUMO of the Pc ring was observed for vanadylphthalocyanine on gold(111). In this case strongly asymmetrical current–voltage traces were obtained due to an enhanced tunneling current detected at positive sample bias.⁸ Although the authors do not discuss the observed band gap of the Pc ring in detail, it appears to be smaller than the gap reported in the literature, which is approximately 2 eV.⁹ Chemisorbed monolayers of α,α' -xylenedithiol on gold have been characterized with STS by Datta et al.¹⁰ Only when the tip is moved far away from the molecule is the expected asymmetry of the current–voltage

* To whom correspondence should be addressed. E-mail address: frans.deschryver@chem.kuleuven.ac.be.

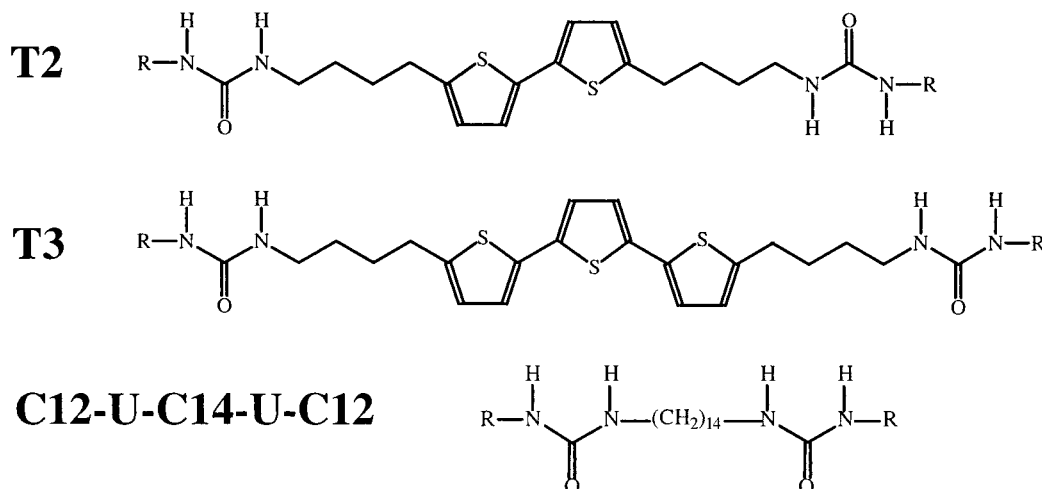


Figure 1. Chemical structure of T2, T3, and C12-U-C14-U-C12. R = C₁₂H₂₅.

characteristics observed. Coronene monolayers have been studied in UHV conditions by Walzer et al.¹¹ *I(V)* curves could be obtained for molecules organized in monolayers on graphite. The curves show a semiconductor band gap that is much less than the calculated value for a free molecule, but an increase with larger tip-sample separation is observed.

Under ambient conditions Stabel et al. studied alkylated hexabenzocoronene molecules physisorbed from solution onto graphite.¹² The current-voltage curves acquired above the alkyl chains are symmetric, while those acquired over the center of the coronene moiety are asymmetric. Onipko et al. measured the *I(V)* characteristics of self-assembled monolayers of conjugated aromatic thiols in air.¹³ They observe an asymmetric shape of the experimentally obtained *I(V)* curves. A series of metalloporphyrin molecules has been investigated with STS at the liquid/gold interface by Han et al.¹⁴ The *I(V)* spectra are found to be characteristically asymmetric due to a noticeable increase in tunneling current at high negative sample bias, especially for the reducible derivatives. This increase is explained by tunneling via oxidized states on the molecule.

Oligo- and polythiophenes form an important class of conducting materials that can find possible applications in, for example, thin film transistors or light-emitting diodes.^{15–17} The two-dimensional ordering of several oligo- and polythiophenes on solid substrates has already been probed with STM.¹⁸ Previous investigations of the bulk properties of the bis(urea)-substituted thiophene derivatives under consideration in this paper have shown that the molecules form one-dimensional (1D) fibers in solution in which the thiophene moieties are π -stacked.¹⁹ Pulse-radiolysis time-resolved microwave conductivity (PR-TRMC) experiments have demonstrated that this arrangement provides an efficient path for charge transport within these self-assembled fibers. Indeed, it has been shown that, by inducing a high degree of molecular order in thin films of oligothiophenes, one can enhance the mobility of charge carriers.²⁰

At this time, we used STM/STS to probe electrical transport through highly ordered self-assembled ribbons of

π -stacked bis(urea)-substituted thiophene derivatives on an HOPG substrate.

The molecular structure of the compounds under investigation is depicted in Figure 1. The synthesis of the compounds has been described elsewhere.^{21,22a} Detailed STM studies on the 2D structure formed by alkyl-substituted bis(urea) derivatives²² and bis(urea) oligothiophenes^{18g} have previously been reported by our research group. Each bis(urea) derivative in a lamella can form up to eight hydrogen bonds with adjacent molecules. Hence a stable and highly ordered supramolecular organization can be observed with submolecular resolution during the STM experiments. Experimental data gathered for the bis(urea) oligothiophenes and theoretical calculations reveal that the thiophene rings are tilted with respect to the surface and have overlapping π -systems. Therefore, further investigation of this system, specifically concerning the electronic properties of the molecules in a 2D adlayer physisorbed on a substrate surface was called for.

Spectroscopic data have been acquired with the STM tip located over the thiophene moieties, but also for the bare HOPG surface and for the alkyl chains of the adsorbed molecules to check the reliability of the resulting *I(V)* curves. The experimentally observed stability of these adlayers and the fact that they are adsorbed on a weak interacting substrate like HOPG ensures that the electronic structure of the molecules we observe in the STS spectra is only slightly distorted by the physisorption process. STS experiments were performed using a Molecular Imaging PicoSPM scanning tunneling microscope controlled by RHK SPM1000 electronics Rev. 7 along with an external pulse/function generator (Tabor Electronics Ltd. Model 8021), with negative sample bias. Tips were electrochemically etched from Pt/Ir wire. Tunneling spectra were acquired with the feedback loop disabled. *I(V)* curves were measured fast (on the order of 100 ms) in order to minimize effects of tip or sample drift during the acquisition of the tunneling spectra. The points where the local *I(V)* curves have been obtained are indicated in the simultaneously obtained STM image. In this way the occurrence of drift in the *x,y*-plane can be identified. The

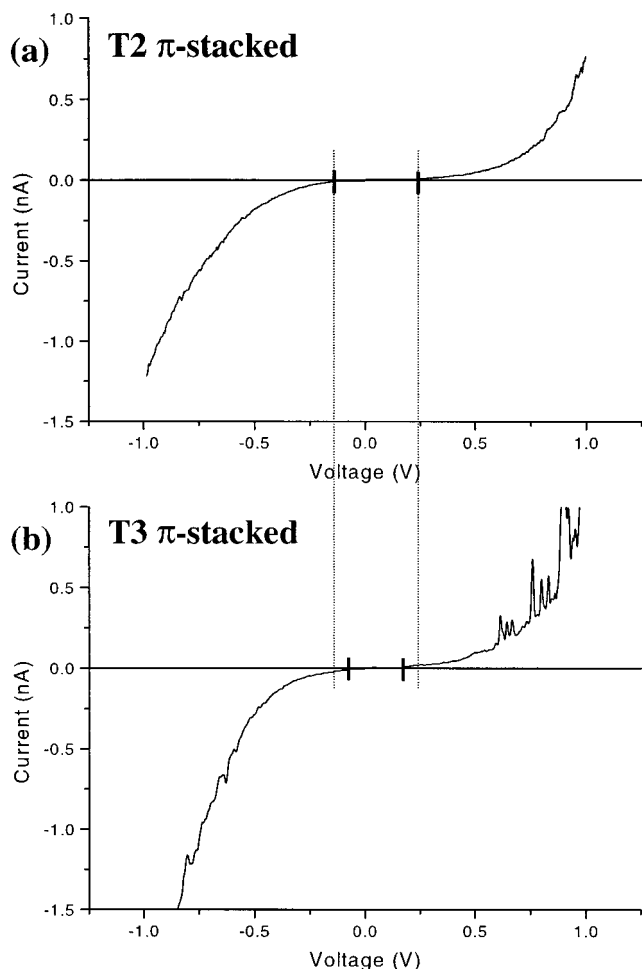


Figure 2. (a) STS curve acquired with the tip located above the thiophene groups of a T2 ribbon. The presented curve is an average over 40 spectra. The band gap observed for T2 in a ribbon is indicated with the solid lines. These lines are also shown in (b) and clearly indicate the different widths of the measured band gaps (dashed lines). (b) STS curve acquired with the tip located above the thiophene groups of a T3 ribbon. The presented curve is an average over 15 spectra. The band gap observed for T3 in a ribbon is indicated with the solid lines.

presented curves are averaged, but not filtered. The acquisition of $I(V)$ spectra proved to be a tedious task. Over 100 curves were obtained for the systems under consideration in order to allow us to identify any possible artifacts. The presented $I(V)$ curves are an average of a selected number of curves that produce the best signal-to-noise ratio for the averaged curve. This was done for clarity. The experimentally observed band gap is defined by a detected tunneling current in the STS spectra that is less than 10 pA, which is the detection limit of the microscope when operated in “standard” current mode.

An averaged $I(V)$ curve obtained above the thiophene moiety of a T2 molecule in a T2 ribbon is shown in Figure 2a. The average is made by acquiring consecutive spectra both over a thiophene ribbon and over several ribbons at different locations in the adlayer. The resulting curve is clearly asymmetric, with higher currents being detected for negative sample bias.¹³ Around the sample Fermi level a small region with suppressed detected tunneling current was

found. Thus, the current–voltage data for T2 reveals semiconductive behavior of the sample. The size of the experimentally observed band gap is 0.45 ± 0.08 eV. The gap is asymmetric around the Fermi level of the sample, pointing out the fact that there exist occupied states of the molecule–substrate complex that are closer to the Fermi level than the unoccupied states of the tip. This proximity of the occupied molecular levels (i.e., HOMO) to the Fermi level of the tip and substrate also opens up the possibility for resonant tunneling, which probably adds to the asymmetry of the $I(V)$ curves. Furthermore, the asymmetric shape observed for the current–voltage curves reported in this paper can also be related to the asymmetry of the tunneling junction. The thiophene adlayer is closer to the substrate than to the tip, taking into account the tunneling parameters used during the course of our experiments. This geometric asymmetry is also reflected in the acquired $I(V)$ curves.

In contrast, the tunneling spectra acquired during the same session over the alkyl chains and those of HOPG do not show a zero-conductance gap around the Fermi level, as shown in Figure 3. Note that these spectra are symmetrical.¹² Reproducibility was good, as demonstrated by the tunneling spectra acquired at different locations over the alkyl chains of the molecules. Figure 3b shows the overlaid curves. To further ensure the reliability of the gathered data, only those $I(V)$ curves were included in the analysis for which we could obtain clear STM images again after the STS measurement. Figure 2b depicts the average of STS curves collected with the tip located over the oligothiophene band in the center of a T3 lamella. Similar as was observed for T2, the tunneling spectra show characteristics of semiconductive behavior. Besides the slightly asymmetric shape of the $I(V)$ curve, a band-gap can be distinguished around E_F , albeit quite small. The size of the measured gap is only about 0.30 ± 0.05 eV, so it is significantly smaller than the band gap observed for the T2 ribbons.

The decrease of the band gap when comparing T2 ribbons with T3 ribbons is attributed to the increased conjugation length, both the intramolecular length and that along the direction of the π -stacked ribbon. Because of this, the gap region around E_F of the T2 ribbons narrows, making the effective semiconductor gap around the sample E_F smaller. Our experimental data are thus in good agreement with previous reports that deal with the relationship between the electronic structure of linear conjugated molecules and their conjugation length.²³ In particular, Brédas et al. did quantum-chemical calculations on conjugated oligomers and polymers.²⁴ They performed an in depth investigation of the importance of interchain interactions in π -stacked systems. When the energy levels of an isolated six-ring thiophene oligomer and a face-to-face stacked dimer were calculated, a clear decrease of the HOMO–LUMO gap was observed in the latter case. For short intermolecular distances in the π -stack the HOMO and LUMO levels of the isolated molecule split and delocalize over the whole π -stacked complex, giving rise to the new molecular states introduced earlier in the discussion.

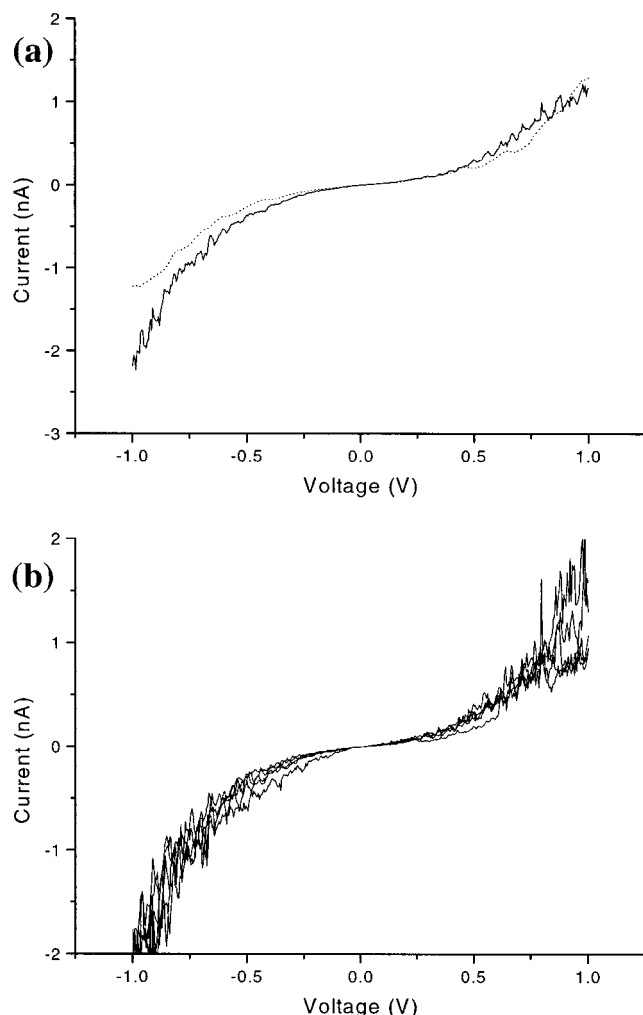


Figure 3. (a) STS curves obtained for HOPG (dotted line) and the alkyl chains of the molecules in a monolayer (solid line). The presented curves are an average over 15 spectra. The curves have a nearly identical shape. No band gap was observed in both cases. The spectrum of HOPG is symmetric. The spectrum of the alkyl chains is nearly symmetric. Only at higher negative bias voltages was a slightly increased current detected for the alkyl chains. (b) Overlaying STS curves acquired over the alkyl chains of the molecules at different locations in a monolayer shows the reproducibility of the measurements.

The experimentally observed band gap for T2 and T3 ribbons is vastly smaller than the bulk semiconductor gaps reported in the literature for polythiophenes (~ 2 eV). This narrowing of the band gap is most likely caused by the proximity of the tip to the sample. The electric field between the tip and sample might significantly influence the electronic structure of the thiophene molecules with regard to their HOMO–LUMO splitting. More importantly, we cannot be sure what the exact tunneling mechanism is. It is, for instance, not certain at all that tunneling actually occurs through the HOMO and LUMO of the molecules. Therefore, assuming that the observed band gap is the HOMO–LUMO gap could be a false assumption. That's why we refer to an experimentally observed band gap rather than to a semiconductor band gap. On top of that, it is at this time not possible to estimate the influence of the presence of solvent on the characteristics of the tunneling junction. The proper way to

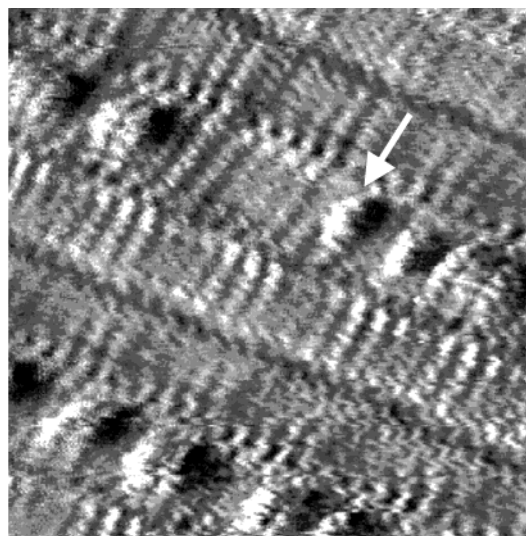


Figure 4. STM image of mixed T2/C12–U–C14–U–C12 monolayers at the 1-phenyloctane/graphite interface. Image size is 10.0×10.0 nm². $I_{\text{set}} = 1.0$ nA, $V_{\text{bias}} = 0.6$ V. Individual T2 molecules can be recognized in the C12–U–C14–U–C12 matrix, as indicated by the arrow.

handle the presented data is therefore to make comparisons between spectra obtained under the same conditions, as proposed in this paper. Because of the distance dependency of the observed band gap, all STS data were obtained with quasi-constant measuring conditions, i.e., a 1 G Ω resistance of the tunneling gap, to avoid large variations in the tip–sample distance.¹¹ When the tunneling gap resistance was increased to 2 G Ω , a widening of the semiconductor band gap of, for example, T3 could be observed (gap size 0.44 ± 0.12 eV at 2 G Ω versus 0.30 ± 0.05 eV at 1 G Ω). This distance dependent behavior can be explained by the proximity of the tip to the surface, probably allowing the electronic states of the tip to perturb the states of the surface. Increasing the tip–sample distance reduces this distortion of the sample electronic states, as reflected in the change of the shape of the tunneling spectra.

To unambiguously confirm the effect of the π -stacking of the oligothiophene units on the observed size of the experimental band-gap of a ribbon, we decided on comparing these data with those for a single T2 molecule. Since it is not possible to image a single isolated molecule physisorbed on HOPG at room temperature with STM, the molecule had to be incorporated into a matrix. To achieve this, mixtures of T2 with C12–U–C14–U–C12 on graphite were measured. We ended up with randomly mixed monolayers, as can be seen in Figure 4. Furthermore, it proved possible to find isolated T2 molecules in the C12–U–C14–U–C12 matrix. Usually, molecules in mixtures tend to form separate domains that are composed of one of the components in the mixture. This has among others been reported for alkane–alcohol mixtures,²⁵ monolayers of fatty acids with different chain lengths,²⁶ mixed alkanol adlayers,²⁷ and unsaturated liquid crystals.²⁸ When C12–U–C14–U–C12 is compared with T2, we find from molecular modeling that their spacers have identical sizes. Thus, the molecules are perfectly compatible and optimal hydrogen bonds between C12–U–

C14–U–C12 and T2 are formed in the mixed adlayer. The hydrogen bond pattern continues along both rows of urea groups in a lamella, and randomly mixed lamellae are formed.

Care was taken that tunneling spectra were indeed acquired over individual T2 molecules. It sometimes occurred that, in the STM image taken after spectroscopic data were collected over an isolated T2 molecule, it was no longer there. In that case the obtained $I(V)$ curve was discarded. Probably, the isolated T2 molecules get expelled from the matrix they are in by the strong electrical field in the tunneling gap during the acquisition of the spectra. The stability of the mixed adlayer itself is quite high. The exchange rate of adsorbed molecules with molecules in the supernatant solution is most probably relatively slow due to the hydrogen bonds between adjacent molecules in a lamella.²⁹ The resulting $I(V)$ curves are shown in Figure 5. As was the case for T2 and T3 molecules in a π -stacked ribbon, the spectra for an isolated T2 molecule exhibit semiconductive behavior. Again, there is a larger deviation of the measured tunneling current from ohmic behavior for negative bias voltages. Below E_F the signal of occupied states becomes apparent starting from -0.30 eV, while above E_F the onset of the signal of unoccupied states occurs at 0.35 eV. Thus, the gap between occupied and unoccupied states is about 0.65 ± 0.11 eV. This band gap is noticeably larger than the gap observed for T2 in a ribbon, meaning that additional states are present closer to E_F for π -stacked T2 molecules, which we feel can only be attributed to the presence of π – π interactions between neighboring T2 molecules in a lamella. Analogous to the comparison between T2 and T3 ribbons, we attribute the decrease of the experimentally observed band gap of a T2 molecule in a ribbon compared to an isolated T2 molecule to the increased conjugation length, in this case along the direction of the π -stacked ribbon.

In conclusion, scanning tunneling spectroscopy is a powerful tool to study electronic properties of molecular systems on surfaces. The electronic properties of the self-assembled structures formed by T2 and T3 have been probed locally with scanning tunneling spectroscopy at the solution/graphite interface. The obtained current–voltage ($I(V)$) curves show a clear zero conductance band gap. The band gap observed for T3 is notably smaller than that for T2. Moreover, when mixtures of T2 with a suitable alkyl-substituted bis(urea) derivative were imaged, it was possible to obtain $I(V)$ curves of an isolated T2 molecule. In this case the observed band gap is considerably larger than for T2 in a ribbon. Thus, these data not only demonstrate, at the molecular level, that the width of the experimentally observed band gap depends on the number of thiophene rings in the molecule but also show that there exists an effective conjugation in the π -stacked ribbons on the surface, which is proven by the narrowing of the experimentally observed zero conductance gap around the Fermi level in comparison to an individual molecule. The controlled arrangement of

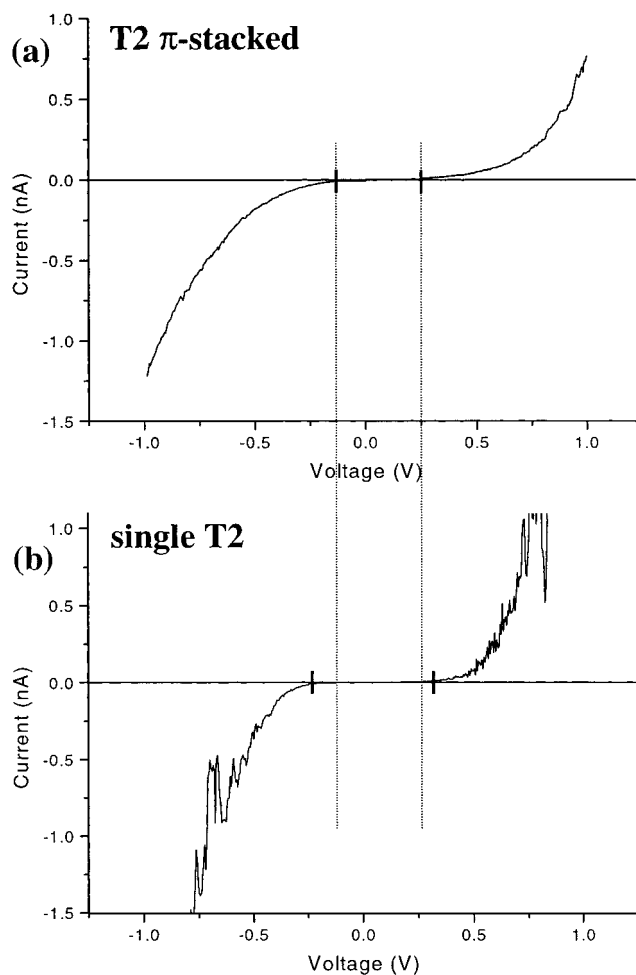


Figure 5. (a) STS curve acquired with the tip located above the thiophene groups of a T2 ribbon. The presented curve is an average over 40 spectra. The band gap observed for T2 in a ribbon is indicated with the solid lines. These lines are also shown in (b) and clearly indicate the different width of the measured band gaps (dashed lines). (b) STS curve acquired with the tip located above the thiophene group of individual T2 molecules in a C12–U–C14–U–C12 matrix. The presented curve is an average over 5 spectra. The band gap observed for an individual T2 molecule is indicated with the solid lines. Clearly, the semiconductor band gap of T2 in a π -stack is significantly smaller than the band gap of a single T2 molecule.

the studied thiophene derivatives could provide a way toward patterning conducting ribbons on a surface on a nanometer scale.

Acknowledgment. We thank the DWTC, through IUAP-IV-11, The Netherlands Organization for Scientific Research (NWO) and Stichting Technische Wetenschappen (STW). The Leuven-Groningen collaboration was made possible by ESF SMARTON. A.G. thanks IWT for a predoctoral scholarship. S.D.F. is a postdoctoral fellow of the Fund for Scientific Research-Flanders. J.v.E. gratefully acknowledges the Royal Academy of The Netherlands for a fellowship.

References

- (1) (a) Avouris, P.; Lyo, I.; Hasegawa, Y. *IBM J. Res. Dev.* **1995**, *39*, 603–616. (b) Ohmori, K.; Ikeda, H.; Iwano, H.; Zaima, S.; Yasuda, Y. *Appl. Surf. Sci.* **1997**, *117–118*, 114–118.

- (2) (a) Feenstra, R. M. *J. Vac. Sci. Technol. B* **1989**, 7, 925–930. (b) Avouris, P.; Lyo, I. *Surf. Sci.* **1991**, 242, 1–11. (c) Hamers, R. J.; Tromp, R. M.; Demuth, J. E. *Phys. Rev. Lett.* **1986**, 56, 1972–1975. (d) Maslova, N. S.; Oreshkin, S. I.; Panov, V. I.; Savinov, S. V.; Depuydt, A.; Van Haesendonck, C. *JETP Lett.* **1998**, 67, 146–152.
- (3) Hess, H. F.; Robinson, R. B.; Dynes, R. C.; Valles, J. M., Jr.; Waszczak, J. V. *J. Vac. Sci. Technol. A* **1990**, 8, 450–454.
- (4) (a) Davis, L. C.; Everson, M. P.; Jaklevic, R. C.; Shen, W. *Phys. Rev. B* **1991**, 43, 3821–3830. (b) Li, J.; Schneider, W.-D. *Phys. Rev. B* **1997**, 56, 7656–7659. (c) Bode, M.; Pascal, R.; Dreyer, M.; Wiesendanger, R. *Phys. Rev. B* **1996**, 54, R8385–R8388.
- (5) (a) Klusek, Z.; Waqar, Z.; Denisov, E. A.; Kompaniets, T. N.; Makarenko, I. V.; Titkov, A. N.; Bhatti, A. S. *Appl. Surf. Sci.* **2000**, 161, 508–514. (b) Collins, P. G.; Grossman, J. C.; Côté, M.; Ishigami, M.; Piskoti, C.; Louie, S. G.; Cohen, M. L.; Zettl, A. *Phys. Rev. Lett.* **1999**, 82, 165–168. (c) Porath, D.; Levi, Y.; Tarabiah, M.; Millo, O. *Phys. Rev. B* **1997**, 56, 9829–9833. (d) Wang, H.; Zeng, C.; Li, Q.; Wang, B.; Yang, J.; Hou, J. G.; Zhu, Q. *Surf. Sci.* **1999**, 442, L1024–L1028.
- (6) Gimzewski, J. K.; Stoll, E.; Schlittler, R. R. *Surf. Sci.* **1987**, 181, 267–277.
- (7) Dekker, C.; Tans, S. J.; Oberndorff, B.; Meyer, R.; Venema, L. C. *Synth. Met.* **1997**, 84, 853–854.
- (8) Barlow, D. E.; Hipps, K. W. *J. Phys. Chem. B* **2000**, 104, 5993–6000.
- (9) (a) Szuber, J.; Szczepaniak, B.; Kochowski, S.; Opliski, A. *Phys. Stat. Sol. B* **1994**, 183, K9–K13. (b) Heilmeyer, G. H.; Harrison, S. E. *Phys. Rev.* **1963**, 132, 2010. (c) Hamann, C. *Phys. Stat. Sol. B* **1968**, 26, 311.
- (10) Datta, S.; Tian, W.; Hong, S.; Reifenberger, R.; Henderson, J. I.; Kubiak, C. P. *Phys. Rev. Lett.* **1997**, 79, 2530–2533.
- (11) Walzer, K.; Sternberg, M.; Hietschold, M. *Surf. Sci.* **1998**, 415, 376–384.
- (12) Stabel, A.; Herwig, P.; Müllen, K.; Rabe, J. P. *Angew. Chem.* **1995**, 107, 1768–1770.
- (13) Onipko, A. I.; Berggren, K.-F.; Klymenko, Yu. O.; Malysheva, L. I.; Rosink, J. J. W. M.; Geerligs, L. J.; van der Drift, E.; Radelaar, S. *Phys. Rev. B* **2000**, 61, 11118–11124.
- (14) Han, W.; Durantini, E. N.; Moore, T. A.; Moore, A. L.; Gust, D.; Rez, P.; Leatherman, G.; Seely, G. R.; Tao, N.; Lindsay, S. M. *J. Phys. Chem. B* **1997**, 101, 10719–10725.
- (15) (a) Carter, F. L., Ed. *Molecular Electronic Devices*; Marcel Dekker: New York, 1982 (Vol. I) and 1987 (Vol. II). (b) *Handbook of Conducting Polymers*; Skotheim, T. A., Elsenbaumer, R. L., Reynolds, J. R., Eds.; Marcel Dekker: New York, 1998. (c) *Conjugated Oligomers, Polymers, and Dendrimers: From Polyacetylene to DNA*; Proceedings of the Fourth Francqui Colloquium; Brédas, J. L., Ed.; De Boeck Universite, Paris, 1999. (d) Friend, R. H.; Gymer, R. W.; Holmes, A. B.; Burroughes, J. H.; Marks, R. N.; Taliani, C.; Bradley, D. D. C.; dos Santos, D. A.; Lögdlund, M.; Salaneck, W. R. *Nature* **1999**, 397, 121–128.
- (16) *Handbook of Oligo- and Polythiophene*; Fichou, D., Ed.; VCH: Weinheim, 1998.
- (17) (a) Horowitz, G.; Bachet, B.; Yasser, A.; Lang, P.; Demanze, F.; Fave, J. L.; Garnier, F. *Chem. Mater.* **1995**, 7, 1337–1341. (b) Burroughes, J. H.; Bradley, D. D. C.; Brown, A. R.; Marks, R. N.; Mackay, K.; Friend, R. H.; Burns, P. L.; Holmes, A. B. *Nature* **1990**, 347, 539–541. (c) Geiger, F.; Stoldt, M.; Schweizer, H.; Bäuerle, P.; Umbach, E. *Adv. Mater.* **1993**, 5, 922–925. (d) Bao, Z.; Lovinger, A.; Brown, J. J. *Am. Chem. Soc.* **1998**, 120, 207–208.
- (18) (a) Bäuerle, P.; Fischer, T.; Bidlingmaier, B.; Stabel, A.; Rabe, J. P. *Angew. Chem.* **1995**, 107, 335–339; *Angew. Chem., Int. Ed. Engl.* **1995**, 34, 303–307. (b) Stabel, A.; Rabe, J. P. *Synth. Met.* **1994**, 67, 47–53. (c) Stecher, R.; Gompf, B.; Muentner, J. R. S.; Effenberger, F. *Adv. Mater.* **1999**, 11, 927–931. (d) Stecher, R.; Drewnick, F.; Gompf, B. *Langmuir* **1999**, 15, 6490–6494. (e) Azumi, R.; Götze, G.; Bäuerle, P. *Synth. Met.* **1999**, 101, 569–572. (f) Vollmer, M. S.; Effenberger, F.; Stecher, R.; Gompf, B.; Eisenmenger, W. *Chem. Eur. J.* **1999**, 5, 96–101. (g) Gesquière, A.; Abdel-Mottaleb, M. M. S.; De Feyter, S.; De Schryver, F. C.; Schoonbeek, F.; van Esch, J.; Kellogg, R. M.; Feringa, B. L.; Calderone, A.; Lazzaroni, R.; Brédas, J. L. *Langmuir* **2000**, 16, 10385–10391. (h) Azumi, R.; Gotz, G.; Debaerdemaeker, T.; Bauerle P. *Chem. Eur. J.* **2000**, 6, 735–744. (i) Mena-Osteritz, E.; Meyer, A.; Langeveld-Voss, B. M. W.; Janssen, R. A. J.; Meijer, E. W.; Bauerle P. *Angew. Chem., Int. Ed. Engl.* **2000**, 39, 2680–2684.
- (19) (a) Schoonbeek, F. S.; van Esch, J. H.; Wegewijs, B.; Rep, D. B. A.; de Haas, M. P.; Klapwijk, T. M.; Kellogg, R. M.; Feringa, B. L. *Angew. Chem.* **1999**, 111, 1486–1490; *Angew. Chem., Int. Ed. Engl.* **1999**, 38, 1393–1397. (b) Rep, D. B. A.; Roelfsema, R.; van Esch, J. H.; Schoonbeek, F. S.; Kellogg, R. M.; Feringa, B. L.; Palstra, T. T. M.; Klapwijk, T. M. *Adv. Mater.* **2000**, 12, 563–566.
- (20) Garnier, F.; Yasser, A.; Hajlaoui, R.; Horowitz, G.; Deloffre, F.; Servet, B.; Ries, S.; Alnot, P. *J. Am. Chem. Soc.* **1993**, 115, 8716–8721.
- (21) van Esch, J.; Schoonbeek, F.; de Loos, M.; Kooijman, H.; Spek, A. L.; Kellogg, R. M.; Feringa, B. L. *Chem. Eur. J.* **1999**, 5, 937–950.
- (22) (a) van Esch, J.; De Feyter, S.; Kellogg, R. M.; De Schryver, F. C.; Feringa, B. L. *Chem. Eur. J.* **1997**, 3, 1238–1243. (b) De Feyter, S.; Grim, P. C. M.; van Esch, J.; Kellogg, R. M.; Feringa, B. L.; De Schryver, F. C. *J. Phys. Chem. B* **1998**, 102, 8981–8987.
- (23) (a) Onipko, A.; Klymenko, Yu.; Malysheva, L. J. *Chem. Phys.* **1997**, 107, 7331–7344. (b) Tyutyulkov, N.; Fabian, J.; Mehlhorn, A.; Dietz, F.; Tadjer, A. *Polymethine Dyes. Structure and Properties*; St. Kliment Ohridski University Press: Sofia, 1991.
- (24) Brédas, J.-L.; Cornil, J.; Beljonne, D.; Dos Santos, D. D.; Shuai, Z. *Acc. Chem. Res.* **1999**, 32, 267–276.
- (25) Venkataraman, B.; Breen, J. J.; Flynn, G. W. *J. Phys. Chem.* **1995**, 99, 6608–6619.
- (26) Hibino, M.; Sumi, A.; Hatta, I. *Thin Solid Films* **1996**, 281–282, 594–597.
- (27) Elbel, N.; Roth, W.; Günther, E.; von Seggern, H. *Surf. Sci.* **1994**, 303, 424–432.
- (28) Stevens, F.; Dyer, D. J.; Walba, D. M. *Langmuir* **1996**, 12, 436–440.
- (29) Gesquière, A.; Abdel-Mottaleb, M. M.; De Feyter, S.; Sieffert, M.; Müllen, K.; Calderone, A.; Lazzaroni, R.; Brédas, J. L.; De Schryver, F. C. *Chem. Eur. J.* **2000**, 6, 3739–3746.

NL015511D